Geophysical Journal International

Geophys. J. Int. (2012) **190,** 981–992 doi: 10.1111/j.1365-246X.2012.05514.x

Sedimentary structure of large sand dunes: examples from Dumont and Eureka dunes, California

N. M. Vriend,[1,*] M. L. Hunt[1] and R. W. Clayton[2]

[1]*Division of Engineering, and Applied Science, California Institute of Technology, Pasadena,* CA 91125, *USA. E-mail: nmvriend@alumni.caltech.edu*
[2]*Division of Geological and Planetary Sciences, California Institute of Technology, Pasadena,* CA 91125, *USA*

Accepted 2012 April 17. Received 2012 April 17; in original form 2011 June 5

SUMMARY

The current research presents ground penetrating radar images up to 30 m in depth of two large desert dunes in California, USA— a barchanoid ridge in the Dumont field and a linear dune in the Eureka expanse. The radar images show a complicated structure of internal layering with ascending cross-strata, cross-bedding and bounding surfaces cutting through layers. Additional research using seismic refraction surveys and sand sampling refine the image of the subsurface (<5 m) structure. The sedimentary structure of the dune shows a strong internal layering with a cemented structure that may immobilize and influence migration of dune expanses. The subsurface features of the sand dune fields in the Mojave Desert provide evidence of dune building, wind regime and precipitation history.

Key words: Ground penetrating radar; Geomorphology; Wave propagation.

1 INTRODUCTION

Short-term climatic changes influence the wind strength, direction and precipitation in a region. The wind affects the appearance and shape of the dune, while precipitation has a direct impact on vegetation on the dune surface and may play a role in the internal structure beneath the surface (Lancaster 1996). The moisture content within a dune in arid regions comes from atmospheric inputs such as rain and humidity and groundwater inputs due to capillary transport (Namikas & Sherman 1995). These factors influence the mobility of a dune field and determine whether a system is dormant and stationary or migrates across the desert plane (Greeley *et al.* 1995).

The long-term climatic profile influences the sediment supply in a region, including particle size distribution and chemical content of the sand (Kocurek & Lancaster 1999). Wind transports sand by saltation, suspension and creep, and prolonged exposed to aeolian environment changes the sorting and shape of the sand grains. The degree of angularity (roundness) reflects the duration of abrasion in the transport of sediments while the sphericity provides an indication of the history of the sedimentary environment (Thomas 1987). The size of sediments in dunes follows as a first approximation a log-normal distribution (Flenley *et al.* 1987). The fine sediments including colloids, clay and silt particles are too small to be carried in saltation by the wind and are removed from the landscape by suspension (Bagnold 1941). Gravel-sized particles and pebbles cannot be transported by saltation and move by impact creep along the surface (Bagnold 1941). The changing topography of dunes limits the interaction of the gravel-sized sediment with the sediment involved with dune building and migration. As a result, the clay and gravel-sized particles are underrepresented in particle size distributions of sediments found near the crest on sand dunes (Livingstone 1987).

Important characteristics of sand dunes are their shape, internal structure and migration speed and direction. These parameters relate to the climatic and depositional environment that create and preserve the dunes and are consequently important indicators for classification of a dune system. Research suggests that large linear dunes do migrate laterally (Livingstone 1987). Research by Livingstone (1987) demonstrates that the crests of a large (∼70 m) linear dune in the Namib Desert shifts back and forth by ∼15 m due to long-term seasonal wind changes. Bristow *et al.* (2007) showed that a net migration of ∼300 m laterally occurred on a longer timescale (∼2500 yr) and posed that large migrations may be temporarily activated or deactivated by long-term climatic changes in rainfall and vegetation.

This paper presents geophysical observations and field measurements of the sedimentary structure of two large desert dunes in the Mojave Desert and connects the observations with the short- and long-term climatic history. Section 2 introduces the regional geologic and climatic setting of the Dumont and Eureka dune field in the Mojave Desert and presents the environmental characteristics and the morphology of the dunes. This research presents measurements mapping the complex internal layering of the dunes in Section 3 with ground penetrating radar (GPR), seismic refraction surveys and sand sampling. The internal structure shows a fascinating snapshot of the dune building and migration characteristics and presents the observer with a look back in time. Section 4 connects the internal structure to the environmental parameters and provides an internal record of major rainfall.

*Now at: Department of Applied Mathematics and Theoretical Physics, University of Cambridge, Cambridge CB3 0WA, UK.

2 REGIONAL GEOLOGIC AND CLIMATIC SETTING

The field areas of this study are in the Mojave Desert, situated between 35°N and 37°N latitude and 116°W and 118°W longitude in the south-western portion of the United States. The arid landscape features several dune systems (Fig. 1a) that originated in the early- and mid-Holocene period (Pavlik 1989). This research focusses on dunes in the Dumont (Fig. 1b) and Eureka (Fig. 1c) dune field.

2.1 Dumont dunes

The Dumont dune field (latitude 35°41′N, longitude 116°13′W) is situated in the northern part of the Mojave Desert in California, USA and was visited on 29 different field days between 2003 and 2009 during the course of this research. The Dumont dune field covers an area of approximately 20 km^2 (MacDonald 1966) near the southern tip of Death Valley. The core of the dune field consist of star dunes surrounded by smaller barchanoid and longitudinal dunes. The highest dune in the centre of the dune field rises 120 m (Nielson & Kocurek 1987) above the desert floor. The dune selected for this research is easy to approach with support vehicles and is near to the northwestern flank of the dune field. The 50-m high dune, shown in Fig. 1(b) is a barchanoid ridge (McKee 1977) with a distinct slip face. Fig. 2 illustrates the general topography of the Dumont dune as measured with a laser rangefinder.

The steep north-facing leeward slope forms when the sand grains blow over the crest and deposit by grainfall. The deposits of grainfall create well-mixed lamination structures that thin downslope (McKee 1977). When sufficient sand is deposited on the upper leeward face, the slope steepens beyond the natural angle of repose of sand (∼30°) and local slope-failure results in grainflow. Grainflow produces cross-strata and inverse grading due to segregation and typically thickens downslope (Hunter 1977). The slope on the leeward face breaks significant at approximately 48 m from the crest forming the transition between grainfall/grainflow and solely grainfall regions. The south-facing side has firmer sand at a shallower slope. This windward slope has a constant slope angle (∼20°) for over 100 m downslope. On most occasions, sand ripples form on the surface of the windward face whereas no ripples are observed on the leeward face.

Seasonal changes in wind direction resulted in changes to the surface features of the dune. For example on 2007 September 18, the brink of the dune was elongated producing a flat region that extended for 30 m to the windward side of the crest. During a visit six months later (2008 March 24), the dune crest had reversed. The lower north-facing slope was slightly shallower than usual at approximately 25°,

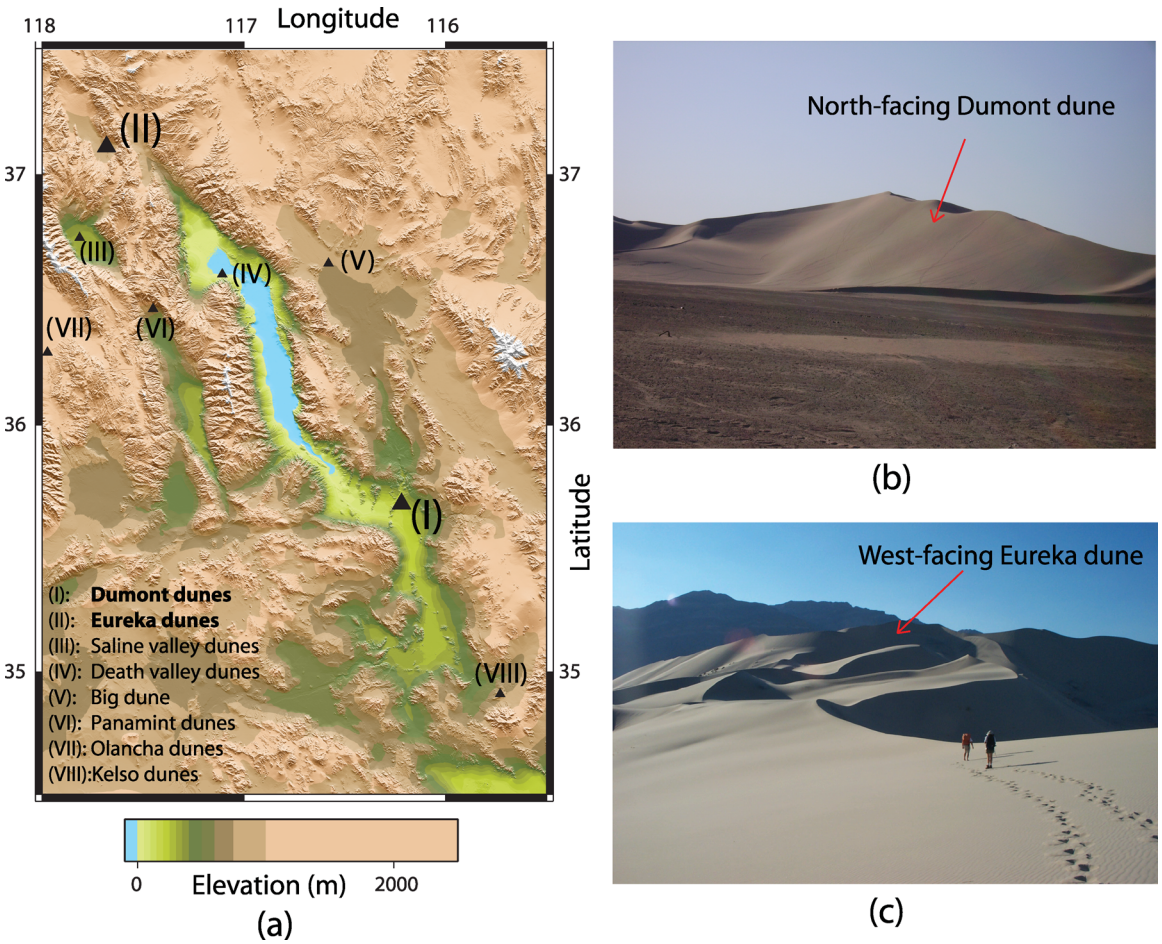

Figure 1. Field locations within the Mojave desert: (a) dunes within the Mojave desert with inserts showing a satellite map of Eureka dunes and Dumont dunes, (b) north-facing (leeward) face of the Dumont Dune, (c) west-facing face of the Eureka Dune.

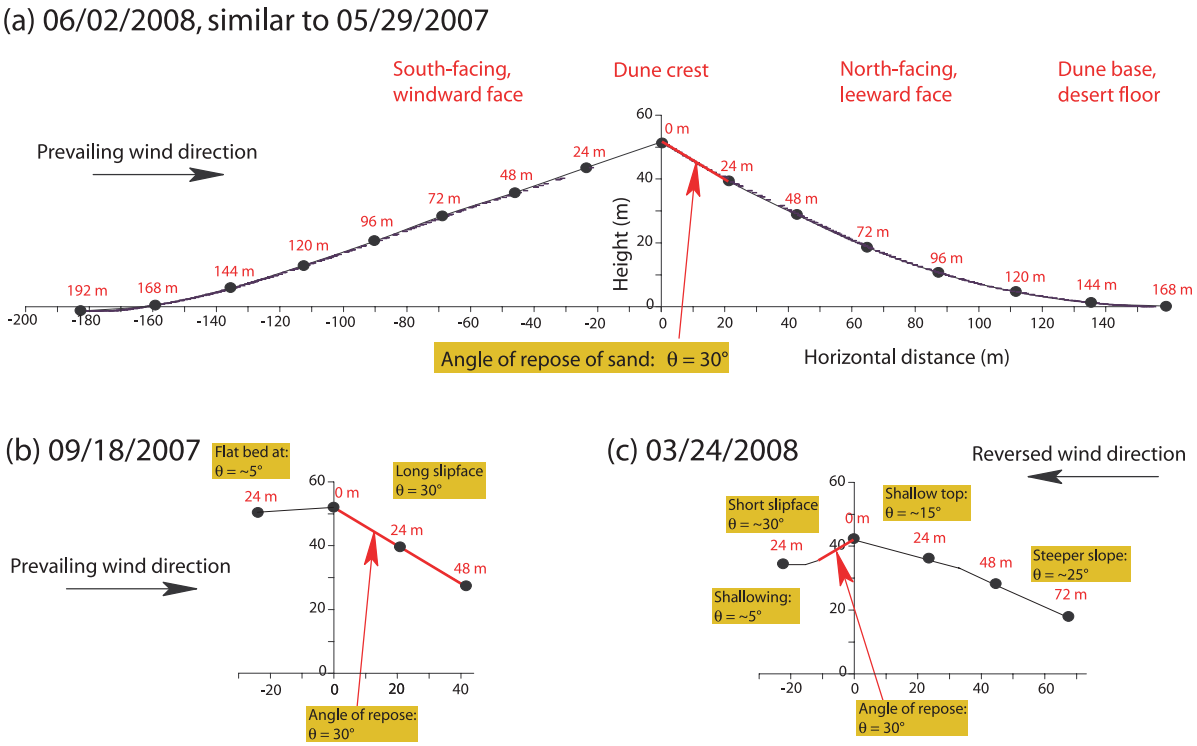

Figure 2. Topography of the Dumont dune measured with a laser rangefinder revealing seasonal changes due to wind regime: (a) 2008 June 2 characterized by a steep leeward north-facing slope and a shallow south-facing windward slope, (b) 2007 September 18 characterized by a longer leeward north-facing slope and a flat south-facing windward slope, (c) 2008 March 24 characterized by a reversed crest due to a prolonged reversed wind direction with a short steep south-facing slope and a shallow north-facing slope.

but the upper north-facing slope was at a constant slope angle of 15° from the crest to 36 m from the crest. Reversal of the crest was observed with a short (14 m) steep slipface on the south-facing slope.

The shape of the dune and the migration characteristics are influenced by the strength of the wind and the variation in directionality. Whether aeolian sediment transport occurs for a given wind depends strongly on the size of the particles (Hunter 1977)—on Earth wind shear velocity higher than 0.2 m s^{-1} for 0.1 mm particles (Bagnold 1941) are of dune building strength. The variation in directionality of the wind influence the type of dune (Hunter 1977). Barchanoid ridges, such as Dumont dunes, are formed when the wind is transverse to the crest with a medium to large sand supply (Wasson & Hyde 1983). The reversed crest observed in the wintertime of 2008 is a manifestation of bimodal winds from the opposite direction. The primary slipface of the barchanoid dune due to the unidirectional wind may be briefly covered by a miniature dune due to the reversing wind. After the normal wind regime has reinstated, the small reversing dune disappears.

Nielson & Kocurek (1987) observed that the wind regime at Dumont dunes differs from season to season. MacDonald (1966) investigated the variation with season by evaluating statistics of dune building winds from the weather station at Silver Lake, California (latitude 35°20′N, longitude 116°05′W), located 40 km SSE from Dumont dunes. Although the Silver Lake weather station is not operational anymore, similar wind regime data is obtained from Mojave River Sink (latitude 35°03′N, longitude 116°05′W, 70 km SSE from Dumont dunes), the closest active weather station to Dumont dunes. The wind rose diagrams for the period 2007 July–June 2008 (Fig. 3) show a strong seasonal variation in wind strength and direction. Calm events, with wind speeds below the velocity threshold of 0.2 m s^{-1}, exist for almost half of the days in the wintertime while the remaining stronger events are from the north. Strong westerly and southerly winds dominate the dune building winds in the summertime. The visual observations of the shape of the dune are in agreement with the governing wind regime from the weather station. The slip-face on the north-faced slope is due to the strong unidirectional wind regime in the summertime. In the wintertime the dune-building winds mainly come from the north and agree with the temporarily reversed dune topography observed in March 2008 in Fig. 2(c). The alternating seasonal wind directions indicate that the dune oscillates slightly during a full year. The net dune migration in NE-direction due to stronger winds in the summertime dominates the migration in S-direction due to calmer winds in the wintertime.

The precipitation events in the desert are short with only a few (1–3) days per month recorded rainfall (Fig. 4a). The annual precipitation varied strongly from ∼30 mm in 2002 and 2006 to ∼150 mm in 2003 and 2005 and most rain fell in February and August. In the summertime, the moisture of the precipitation evaporates readily when the average temperature rises well above 35 °C and average maximum daytime temperatures tops 45 °C (Fig. 4b). The average temperature drops to 10 °C in the wintertime, which reduces the potential to drive moisture out of the dune.

2.2 Eureka dunes

Eureka dunes (latitude 37°07′N, longitude 117°41′W) are situated in Eureka Valley in the northern part of Death Valley National Park in California, USA and were visited on six different field days in 2002, 2007 and 2008 during the course of this research. The highest peak

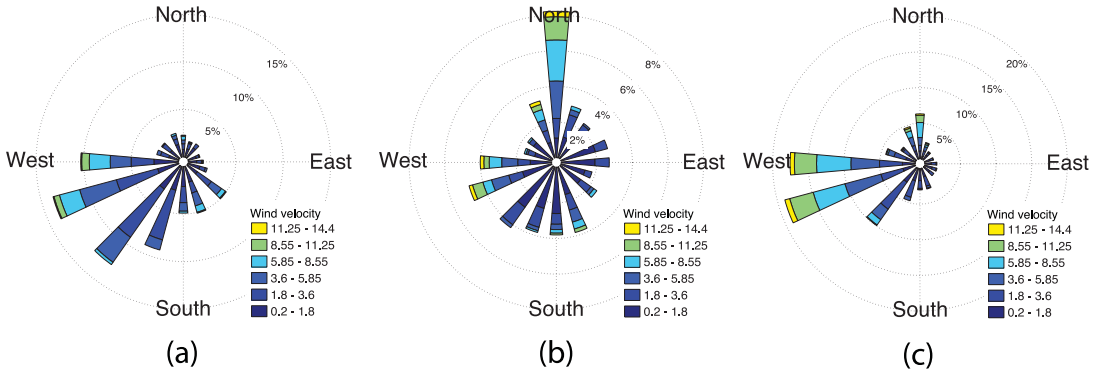

Figure 3. Wind rose diagrams for Mojave River Sink (70 km SSE from Dumont dunes) from data from the Western Regional Climate Centre: (a) 2007 July–October with 20.8 per cent calm events, (b) 2007 November–2008 February with 45.2 per cent calm events, (c) 2008 March–June with 14.9 per cent calm events.

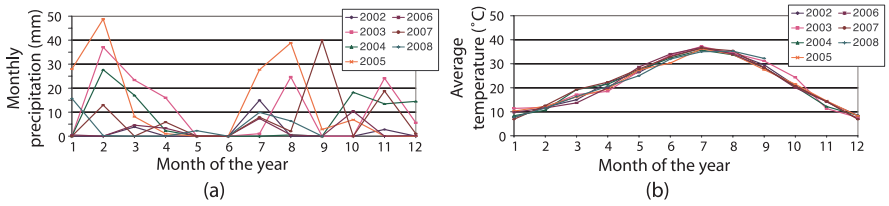

Figure 4. Environmental data collected from Mojave River Sink (70 km SSE from Dumont dunes) from data from the Western Regional Climate Centre: (a) Monthly precipitation for 2002–2008, (b) monthly average temperature for 2002–2008.

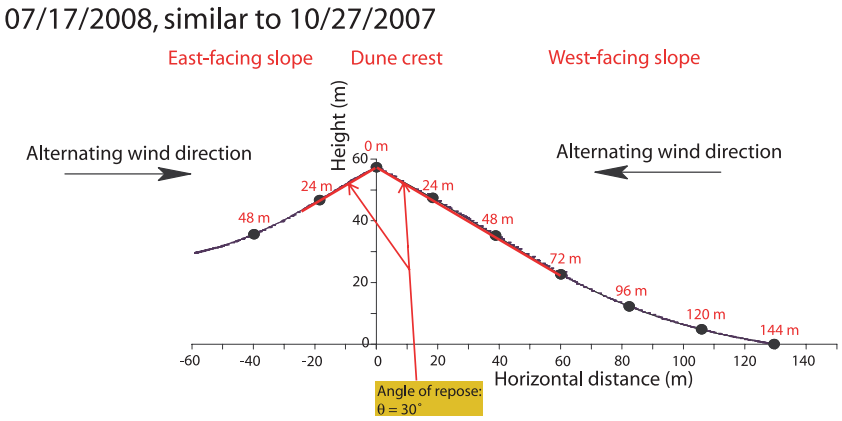

Figure 5. Topography of the Eureka dune on 2008 July 17 measured with a laser rangefinder characterized by steep slipfaces on both the east- and west-facing slope.

of the Eureka Dune system rises about 200 m above the surrounding valley floor. Several type of dunes are superimposed on top of each other in the dune field. The dune selected for this research is a linear dune and rises 60 m above the surrounding dunes (Fig. 1c). Fig. 5 illustrates the general topography of the Eureka dune as measured with a laser rangefinder.

The east-facing and west-facing surfaces are both at the angle of repose for 30 m on the east-facing slope and for 72 m on the west-facing slope. The characteristic dual slip face structure of linear dunes, such as the Eureka dune in the current study, is a result of winds from two directions (McKee 1977). This bimodal structure indicates a complicated wind regime with common reversals of prevailing dune building winds.

The Eureka dune expanse lies at the southern end of the Eureka Valley. The shape of Eureka Valley funnels the wind such that sand is deposited against its southern end where the valley ends in the Last Chance Mountains. No active weather stations are located in the nearby region and therefore information on prevailing wind directions and precipitation is sparse. The average precipitation from long-term climate data is 115 mm per year (Pavlik 1980) with most of the rain falling between November and March; similar to Dumont Dunes, there may also be thunderstorms in July and August. The summer daily temperatures exceed 40 °C between June and August and the minimum temperature between November and March may drop below the freezing point.

3 INTERNAL STRUCTURE OF A DUNE

The internal structure of sediments in a sand dune are commonly exposed by the physical and time-consuming process of digging trenches and examining the deposits (McKee 1977; Nielson &

Kocurek 1987). Although trenching can show a complex internal structure with layering and bounding surfaces, only one discrete location is examined at a time. By contrast, near-surface geophysical techniques may be used to investigate and map the subsurface structure of a sand dune along large distances and provide a continuous measurement of discrete layers within a dune.

GPR surveys are a well-known technique to investigate the structure of sand dunes (Schenk *et al.* 1993; Bristow *et al.* 2000;

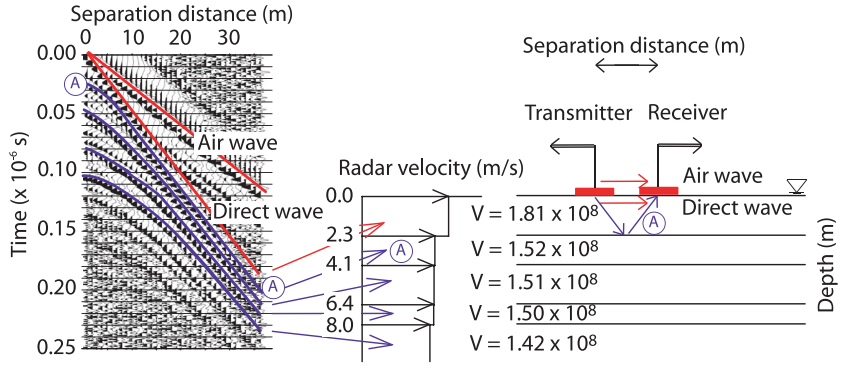

Figure 6. Common-midpoint gather of a survey with a 200 MHz antenna at Dumont dunes on 2007 September 18. The transmitting and receiver antennas are separated by an additional 1 m for each trace. The air and direct wave are straight lines in the shot record and have a velocity of 300×10^6 m s^{-1} and 181×10^6 m s^{-1}, respectively. The reflection hyperbola originate from discrete layers within the subsurface—the curvature determines the radar velocity and the intersection with the origin sets the depth of the layer.

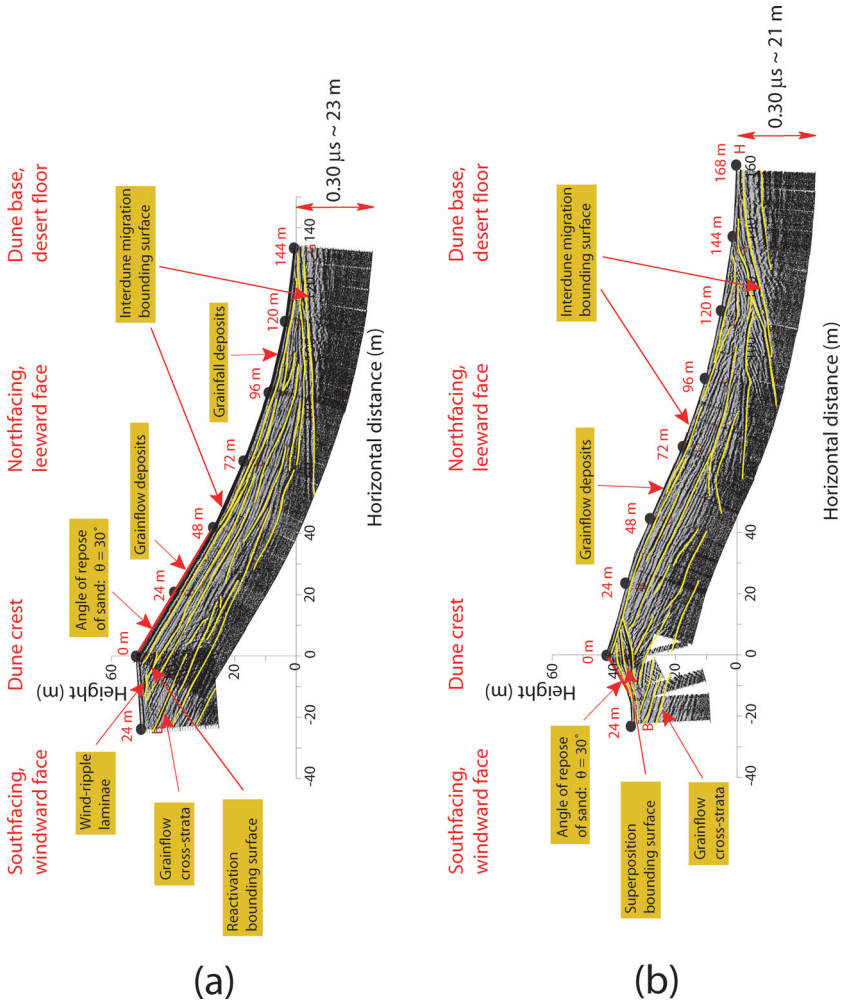

Figure 7. Internal structure of the Dumont dune measured with 100 MHz ground penetrating radar: (a) 2007 September 17, characterized by grainflow cross-strata and deposits and (b) 2008 March 24, characterized by a strong superposition bounding surface. The profile is scaled with the radar velocity such that the time coordinate is approximately equal to the spatial coordinate. The yellow lines follow the local reflection profiles and are added for interpretation.

Grandjean *et al.* 2001). Radar surveys show a comprehensive image of the subsurface structure and supplement observations of surface features. Earlier work by Vriend *et al.* (2007) investigated the subsurface structure of a dune with seismic refraction experiments and observed sharp jumps in velocity in depth. However, seismic surveys only provide point measurements of the internal structure, as depth of the layer can only be approximated due to a large uncertainty in traveltimes. The current research presents a comprehensive analysis of the sedimentary structure of the subsurface by combining the internal structure obtained from GPR surveys and the velocity structure measured with seismic surveys. Sand sampling provides a direct measurement of the local composition and water content and complements the image of the near-surface structure of sand dunes.

3.1 Ground Penetrating Radar

GPR surveys are conducted with a PulseEkko 100 system with two different antennas. The 100 MHz antenna penetrates deeper in the dune, up to 30 m at Dumont and up to 40 m at Eureka dunes, depending on local dielectric properties. The 200 MHz antenna provides a better resolution near the surface of the dune, but has a shallower penetration. The contrast in a radargram is created by reflection of waves of interfaces due to a changing radar velocity. This radar velocity depends on the dielectric material properties and may change slightly between different field dates, due to moisture content. The radar velocity is obtained from a common-midpoint (CMP) survey obtained around a point 24 m on the leeward face of the dune and decreases from 181×10^6 m s^{-1} at the surface to 142×10^6 m s^{-1} at a depth of 8.0 m, as illustrated in Fig. 6.

The results of the radar profiles for four different field experiments at Dumont are presented in Fig. 7 for the 100 MHz antenna providing deeper penetration and Fig. 8 for the 200 MHz antenna resulting in shallower penetration with a higher subsurface resolution. The structure on the leeward face is dominated by parallel layers at the angle of repose in the upper regions of the dune. The slope on the leeward face breaks significantly at a point between 24 and 48 m from the crest and forms the transition between grainflow and grainfall regions. A thickening in the structure occurs at the transition between the grainfall and grainflow region and the layers become irregular and thin near the base of the dune. The desert floor shows up distinctively in the radar profile as a horizontal layer that slightly dips underneath the dune itself and the base of the dune has rich cross-bedding. The structure on 2008 March 24 shows a flattened crest with strong cross-bedding penetrating the upper part of the leeward slope. Visual observations of the surface on the windward face do not indicate any change in structure penetrating through the surface. The internal structure from radar profiles, however, shows strongly dipping layers, at an angle of $\sim 30^\circ$, penetrating up to the surface of the windward face. This cross-bedding is a direct result of migration of leeward faces in the downwind direction.

The results of the 200 MHz profiles for two different field experiments at Eureka are presented in Fig. 9. Strong subsurface parallel layering characterizes both the west- and east-facing slope on 2007 October 27. At the location where the slope breaks significantly the layering thickens and new layers appear closer to the surface. The radar profile of the east and west face on 2008 July 17 show continuous thinning downslope, very similar to the structure observed by Bristow *et al.* (2000) for linear sand dunes. Extensive cross-bedding occurs throughout the entire profile. The horizontal 'supersurface' bounding surface (Kocurek 1996) is evidence of eroded and buried

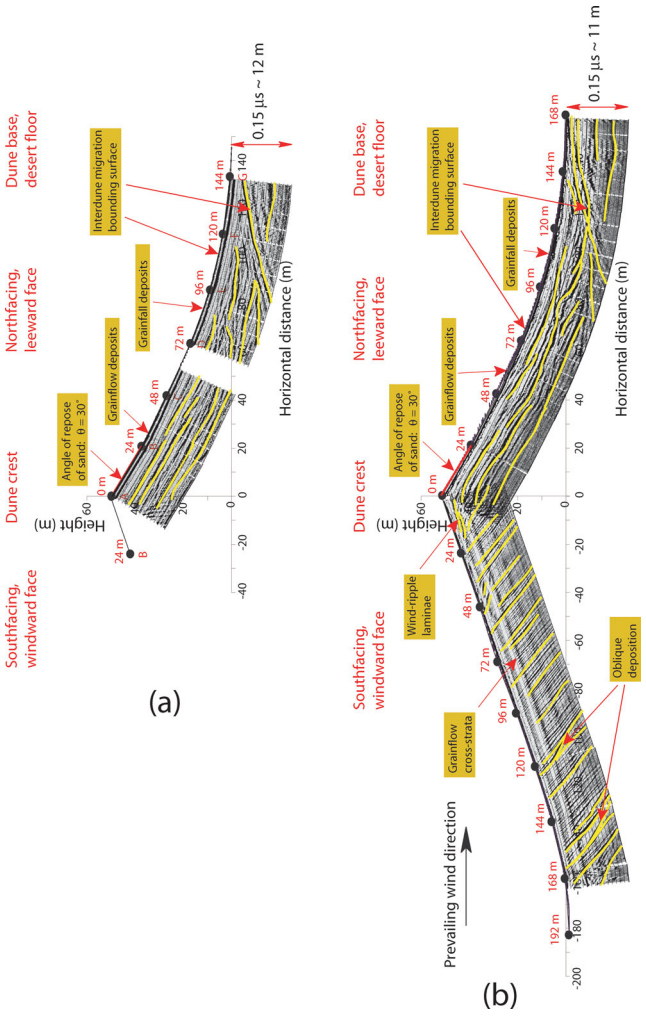

Figure 8. Internal structure of the Dumont dune measured with 200 MHz ground penetrating radar: (a) 2007 May 29, characterized by grainflow cross-strata and deposits and (b) 2008 June 2, characterized by continuing grainflow cross-strata along the entire length of the windward face. The profile is scaled with the radar velocity such that the time coordinate is twice the spatial coordinate. The yellow lines follow the local reflection profiles and are added for interpretation.

compound dunes. Most notable is the very strong reflection of a buried dune crest in Fig. 9(b) at approximately 115 m from the crest.

Kirchhoff migration (Reynolds 1997) on GPR profiles has been applied to translate the time dimension to a spatial dimension. The complex dune structure is resolved to a depth of over 30 m for the 100 MHz antenna, as illustrated in Fig. 10. The migrated figures show several internal crests that oscillate slightly between west and east with depth. The stars in Fig. 10 indicate the position of the internal crests.

3.2 Near-surface velocity and sedimentary structure of a dune

Vriend *et al.* (2007) investigated the compressional seismic velocities of the subsurface structure of dunes in detail with seismic refraction surveys and observed sharp jumps in velocity with depth

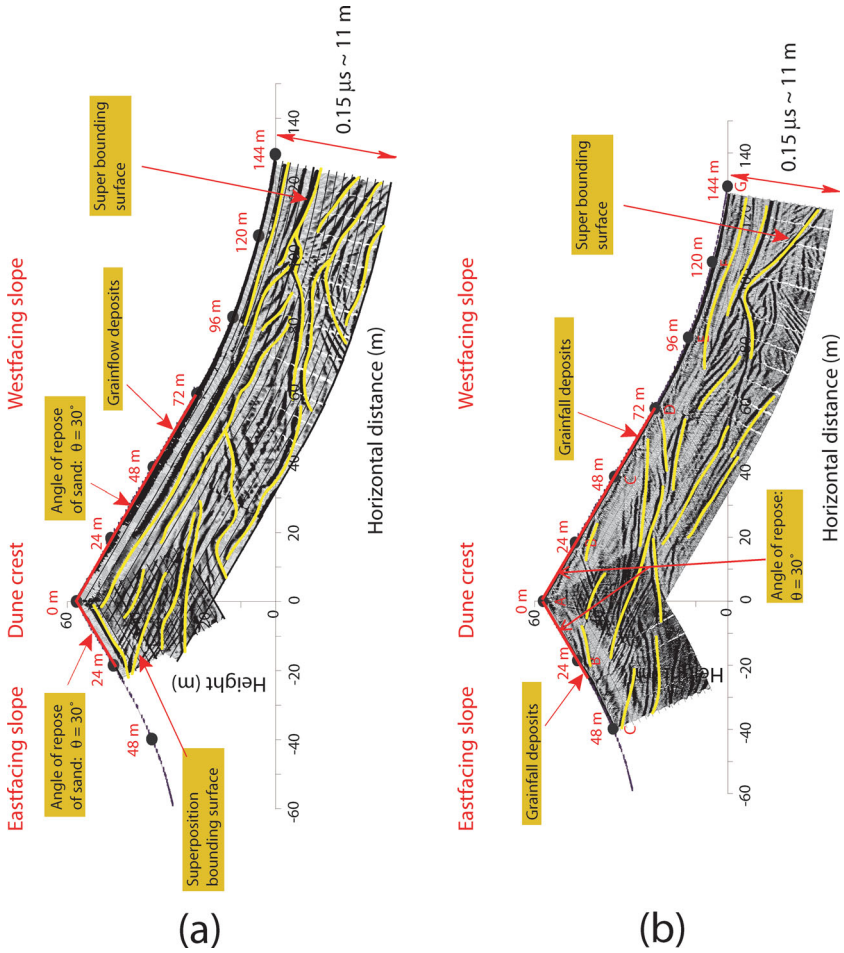

Figure 9. Internal structure of the Eureka dune measured with 200 MHz ground penetrating radar: (a) 2007 October 27 and (b) 2008 July 17, both characterized by a rich internal structure. The profile is scaled with the radar velocity such that the time coordinate is twice the spatial coordinate. The yellows lines follow the local reflection profiles and are added for interpretation.

and a strong lateral gradient in velocity in downhill direction. Combining the seismic velocity structure of the dunes with the ground penetrating radar profiles provides a comprehensive view of the subsurface structure. The wave propagation characteristics of the seismic refraction experiment have been analysed in further detail. Both the body *P*- and *S*-wave and the surface Rayleigh wave are present in the shot record resulting from a broad-band hammer impact. Waves are travelling from the impact source along an array of 48 geophones. The velocity increases due to compaction and moisture content as the waves penetrate deeper into the dune for the farthest sensors from the impact. An example of a shot record is presented in Fig. 11 for a field experiment at Dumont dunes on 2007 May 29. The refractive analysis shows a near-surface layer of 180 ± 20 m s^{-1} on top of a faster layer of 300 ± 30 m s^{-1} that is on top of a half space of 350 ± 30 m s^{-1}.

Fig. 12 shows the near-surface section of the radar profiles for the four different field dates on the leeward face at Dumont dunes, complemented with velocity data for two available field dates. The 2007 May profile in Fig. 12(a) shows a layer materializing close to the crest of the dune and continuing to 33 m where it dips down into the deeper sections of the dune. The velocity structure features an increasing seismic velocity and a thickening layered structure in the downhill direction characteristic of grainflow processes. The 2007 September profile in Fig. 12(b) presents a deep and irregular layering close to the crest, but well defined and closer to the surface in a region from 27 to 48 m from the crest after which it dips deeper into the dune. Furthermore, the strong radar reflection also appears slightly earlier in the record indicating a shallower layer in September. The subsurface structure in the upper section is characteristic of grainfall processes as it thins in downhill direction. The 2008 March data show strongly tilting layers oriented at an angle steeper than the surface, indicating that the layers were formed at the angle of repose and eroded off when the surface of the dune attained a shallower angle. The radar profiles indicate strong cross-bedding parallel to the angle of repose and reversed layering near at the crest. The leeward face is at a shallower angle than usual (Fig. 2) and the crest is topped off (Fig. 12c) indicating that the original layering remains but is now in a tilted orientation with respect to the surface. The 2008 June profile in Fig. 12(d) reproduces a situation very similar to the 2007 May data, a distinct subsurface layer at the upper part of the dune, between 10 and 24 m, that dips deeper close to the crest and further downhill.

Fig. 13 presents the near-surface section of the radar profiles for the two different field dates at Eureka dunes. The 2007 October profile in Fig. 13(a) shows a parallel layering on both sides of the dune near the surface with tilted layering deeper in the dune. The seismic velocity increases downhill on the west-facing slope and the east-facing slope features a significant higher seismic velocity than the opposite side. In contrast, the 2008 June data presented in Fig. 13(b) illustrate strongly tilted layering of the subsurface

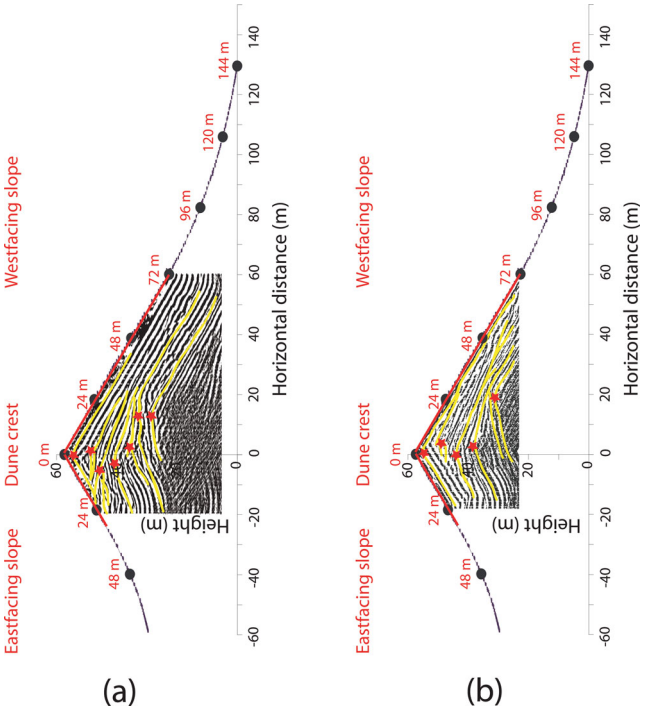

Figure 10. Kirchhoff migrated ground penetrating radar data of the Eureka dune on 2007 October 27 for 100 and 200 MHz data.

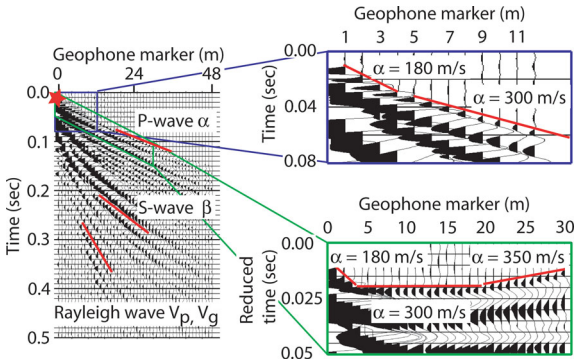

Figure 11. Shot record of the seismic refraction experiment of the Dumont Dune on 2007 May 29. The array of 48 geophones are laid out perpendicular from the crest in the direction of the base of the dune with a spacing of 1 m. The impulse at position zero provides energy needed for the seismic refraction experiment. The first insert and second insert show details of the internal refraction of the first arrival *P*-waves, illustrated with distinct breaks in the slope.

structure on both sides of the crest, extending to the surface, resulting in an irregular near-surface layering.

Table 1 summarizes the radar velocity V_r and two-way traveltime t_0 measurements and calculates the distance to the first large reflector. The shortest distance from the surface to this subsurface layer H varies between different field dates. The error margins are obtained with an error of $\delta t = 0.0005\ \mu$s and $\delta V_r = 5 \times 10^6\ \mathrm{m\,s^{-1}}$. The environmental parameters such as precipitation, temperature and wind regime differ throughout the season and therefore differences in velocity and general structure are observed. However, the subsurface layering persist even through large reversals of the wind direction and therefore the layers parallel to the angle of repose remain at that orientation in Fig. 12(c). This indicates that the

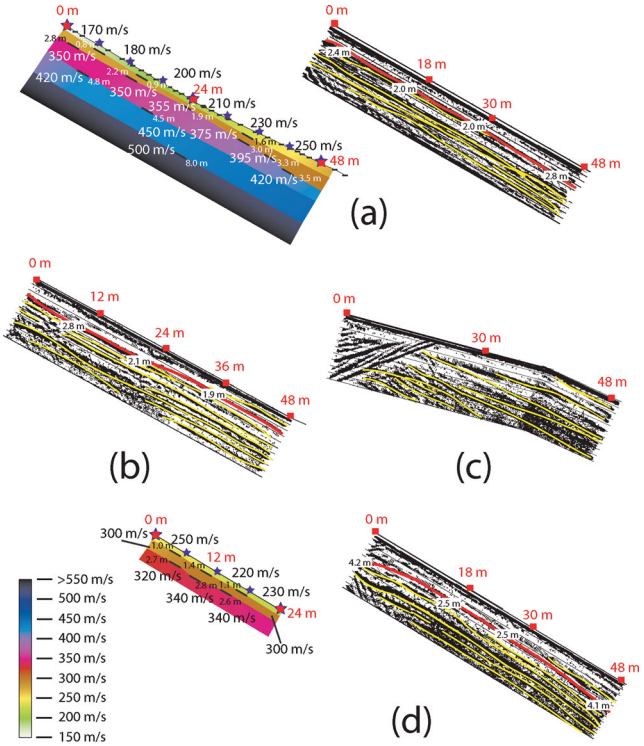

Figure 12. Near-surface velocity structure and internal layering of the Dumont dune: (a) GPR and seismic of 2007 May 29, (b) GPR of 2007 September 18, (c) GPR of 2008 March 24, (d) GPR and seismic of 2008 June 01. There is some variation in near-surface layering throughout the season, but the general characteristics remain the same.

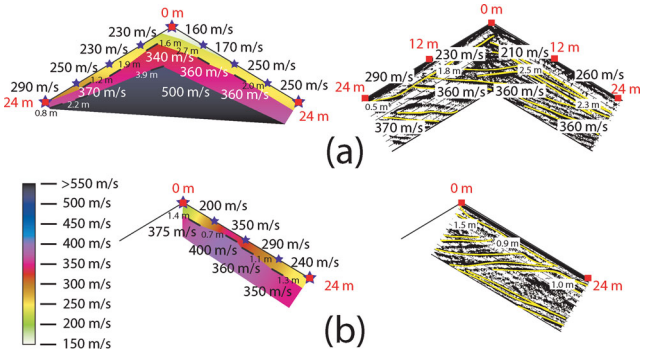

Figure 13. Near-surface velocity structure and internal layering of the Eureka dune: (a) GPR and seismic of 2007 October 27 featuring near-surface parallel layer on both faces with deeper tilted layers and (b) GPR and seismic of 2008 July 17 showing strongly tilted layers penetrating to the surface.

subsurface structuring at the angle of repose persist throughout the year.

3.3 Sand sampling

Sand sampling is critical in explaining the underlying reasons for the strong sedimentary structures in the dune observed by ground penetrating radar and the large velocity increase across the structure as observed from seismic profiling. A Raman spectroscopy measurement shows that the Dumont sand is composed of quartz and K- and Na-feldspar components. A x-ray fluorescence

Table 1. Ground penetrating radar survey results at Dumont and Eureka Dunes, performed with the 200 MHz antenna.

Location & Date	Survey	V_r (m s^{-1})	t_0 (s)	H $\pm$ δH (m)
Dumont & 2007 May 30	North face	1.73×10^8	23×10^{-9}	2.0 ± 0.10
& 2007 September 18	North face	1.81×10^8	21×10^{-9}	1.7 ± 0.10
& 2008 March 24	North face	1.61×10^8	tilted	–
& 2008 June 02	North face	1.65×10^8	30×10^{-9}	2.5 ± 0.12
Eureka & 2007 October 28	West face	1.73×10^8	27×10^{-9}	2.3 ± 0.11
& 2007 October 28	East face	–	21×10^{-9}	1.8 ± 0.10
& 2008 July 18	West face	1.69×10^8	tilted	–
& 2008 July 18	East face	–	tilted	–

measurement of Dumont sand quantifies heavier chemical elements ($Z > 11$) and shows in the crest sand a large component of silicium (32.66 per cent) and intermediate quantities of aluminium (6.04 per cent), natrium (3.08 per cent), potassium (2.92 per cent) and calcium (2.20 per cent). The sand from the base of the dune has similar major components, but less calcium (1.90 per cent).

From a granular point of view, a more interesting feature of sand is its distribution of particle sizes. Livingstone (1987) investigated 325 samples collected from 25 sites on a linear dune in the Namib desert over a period of a year and concluded that changes in size distribution are gradual and have a seasonal variation. The crest samples are finer, better sorted and less skewed than samples from the dune base. If the grains originate from one population, the sand may be approximated by a log-normal distribution with a characteristic average diameter and standard deviation (Flenley *et al.* 1987). Analysis of surface samples taken from a Dumont dune at different positions from the crest (Fig. 14) shows that the average particle size is nearly constant along the dune, but that the standard deviation increases strongly on the windward face and beyond 30 m from the crest on the leeward face. These results are in agreement with the trend of mean grain size as presented in Livingstone (1987).

To obtain information on the grain sizes and moisture content internal to the dune, a sampling probe slightly longer than 2 m was designed and constructed. The tip of the probe captures approximately 16 g of sand at a certain depth that is locked in an air-tight container and brought to the laboratory for further analysis. The probe is inserted vertically and collects a sample perpendicular to the surface at a depth of cos (30°) times the length of the probe. The moisture content, expressed as the percent by weight (Namikas & Sherman 1995), strongly increases with depth. In the summertime, the water content in sand is ∼0.1 per cent close to the surface and gradually increases to 1 per cent at a penetration depth of 1.75 m. In the wintertime, the moist (∼0.5 per cent) dune features a concentrated near-surface layer at a depth of 0.2 m with a high water content (2 per cent) and a wet (3 per cent) layer at a depth of approximately 1 m. Experimental research reported in Namikas & Sherman (1995) indicates that surface moisture levels exceeding 1 per cent can significantly limit the sand transport due to increased cohesion between the sand grains.

A very hard, concrete-like layer exists at the leeward face of the Dumont dune around a depth of 1.5–2 m, which has been highlighted in Fig. 12 in red. The sampling probe could not be forced through this layer. Upon extraction of the probe, small conglomerates of sand were discovered in the sample, as illustrated in Fig. 15. These conglomerates consist of approximately 5–10 sand grains across and are linked together with a binding cement. The cement does not dissolve in water and the sand remains bonded. These conglomerates have been found for three different field dates when sufficiently deep samples were collected: at a depth of 1.3 m and 20 m from the crest on 2005 July 2005; at a depth of 1.3 m at 35 m from the crest on 2005 September 08; and at a depth of 1.6 m and 36 m from the crest on 2007 July 16. Because of the point-wise character of the measurement, the extent of the layer and variation in depth between field dates is not known.

A scanning electron microscope analysis shows that the cement between individual grains is calcite $CaCO_3$ and dolomite $CaMg(CO_3)_2$, mixed with clay-sized particles. The cementation of the sand grains likely results in a decrease in porosity and a strong increase in velocity. Sand sampling at various depths shows that the strong sudden increase in seismic velocity as observed in Vriend *et al.* (2007) is due to an abrupt occurrence of these cemented layers at a certain depth.

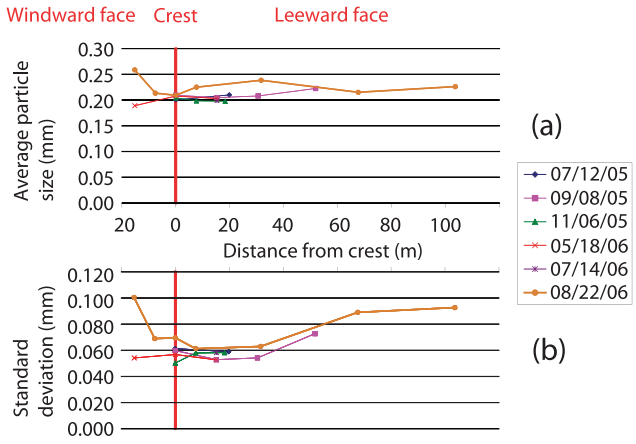

Figure 14. Particle characteristics of a surface sand sample from Dumont dunes: (a) average particle size, (b) one standard deviation. The windward face of the dune is on the left-hand side of the crest, while the leeward face of the dune is on the right-hand side of the crest.

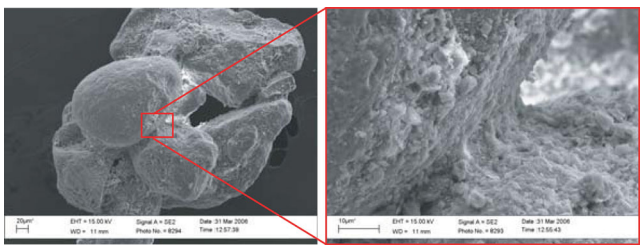

Figure 15. Sand conglomerate obtained from a sample 1.3 m deep and 20 m from the crest on the leeward face at Dumont dunes on 2005 July 12.

4 DISCUSSION ON THE SEDIMENTARY STRUCTURE

The calcium necessary for the cementation needs to be available at a depth of approximately 1.5 to 2 m from the dune surface, as highlighted in Fig. 12. This calcium may be provided by dust, rain or from internal water flow. If the calcium was provided with internal water flow, the capillary draw needs to be very strong to supply water from the ground level to a height of approximately 40 m. Large bodies of free-surface water are not available for all dunes, although some dunes border large rivers (Golden Bell of Resonant Sand, near Shapotou, China) and interdune lakes (Badain-Jaran dunes, China; Dong *et al.* 2003). Rainfall may supply the minerals necessary for cementation and calcium is an important component in the precipitation in the Mojave Desert (∼8 mg/L in spring 2002, National Atmospheric Deposition Program). Another possibility is that desert dust provides the necessary calcium and is percolated into the dune by precipitation or seepage (Louge *et al.* 2010). The supply of $CaCO_3$ from dust for subsurface cementation in the southwestern USA has been shown and documented by Reheis *et al.* (1995). Clay-sized particles and an excess calcium source create the bonding material. When precipitation percolates through the dune, it supplies the minerals and clay-sized particles needed for this process. Sand at the surface of the dune has shortage of clay-sized particles ($D = 0.001$–0.0039 mm) as deduced from sieving experiments and this particle size may have transported down into the dune.

Subsurface cementation has been reported in literature for various sediment type: including sandstone, subaqueous, aeolian and Antarctic dunes. MacKenzie (1964) recognized strong bedding due to calcareous surface cementation in Bermuda sandstone. The author suggested that percolating rainwater induces rapid surface cementation, provides stabilization and preserves the structure. Slow stabilization leads to erosion and cross-bedding on the windward face of the dune, similar to the structure on the windward face of Dumont dunes. Flemming & Bartoloma (1995) collected core samples of sand in marine deposited dunes and observed strong cross-bedding and cementation at 1.9 and 3.0 m depth. The authors noticed that the cementation occurred after a layer has been buried below a critical thickness of sediments and does not form on the water-sediment interface. Dong *et al.* (2003) recognized cementation in large megadunes in the Badain-Jaran desert and argued that vegetation and cementation by calcium deposits promotes dune fixation. Subsurface ice-cemented layers in sand and snow Antarctic dunes may strongly influence the humidity balance between snowmelt and vapor transfer and fixate dunes temporarily (Calkin & Rutford 1974).

The regular subsurface pattern on the windward face of the Dumont dune shows dipping layers close to the angle of repose. Closer to the desert floor on the windward face are a few intersecting layers that are oriented at a shallower angle. These second-order surfaces were formed when the dominant wind blew from a different direction, therefore creating a slipface at an oblique angle compared to the current topography (Kocurek 1991). The individual layers are separated from each other with a spacing of approximately 2 m. Fig. 16(a) presents a discretization of the layers, in which the amplitude represents the strength of the layer in the GPR profile. Fig. 16(b) provides an estimate of the relative annual precipitation. The raw data has been provided by Dr. Richard Hereford (USGS Flagstaff, Arizona) in personal communication and includes average precipitation records of 52 Mojave desert weather stations. The mid-century dry period between 1945 and 1977 is the most

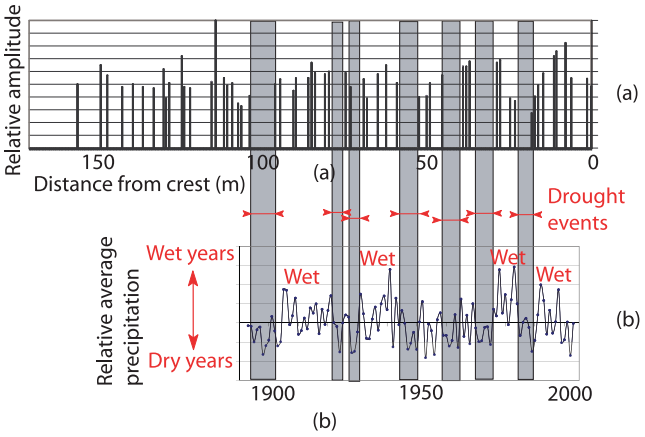

Figure 16. Correlation between layering and long-term precipitation: (a) Discrete representation of the layering on the windward face of Dumont dunes from GPR measurements, (b) Relative annual precipitation for 1890–2000. Long term environmental data is collected from averaging precipitation records from 52 Mojave desert weather stations shared by Dr. Richard Hereford (USGS Flagstaff, Arizona) in personal communication. The grey bars indicate drought events.

distinct feature in the precipitation records (Hereford *et al.* 2006) and is linked to a section along the dune without significant layer formation.

The dune migrates approximately 1 m a year based on the correlation between appearance of significant layering and large precipitation events. The weakness in the one-to-one comparison is that a constant migration speed may not be present. Wet years may freeze or slow the migration speed and not acceleration or deceleration is taken into account. In future work, a more accurate estimate of the migration rate, together with insights on the time-dependent feedback of precipitation on migration, may be obtained with optically stimulated luminescence dating (Bristow *et al.* 2005) of sand samples.

5 CONCLUSIONS

This study connects the internal structure of a Dumont and Eureka dune in the Mojave desert to environmental characteristics. The wind strength and direction influences the shape of sand dunes from season to season. The deployment of ground penetrating radar is an efficient method to image the subsurface structure and provides a continuous interpretation of the dune's sedimentary structure up to a depth of 30 m. Cross-bedding and regular layering, as revealed by ground penetrating radar surveys, are a direct result of grainfall, grainflow and other sedimentary processes in dune building dynamics. Subsurface sand sampling identifies a compacted and solidified layer at regular intervals. The layering occurs for the Dumont dune in a random pattern that correlates with large precipitation events providing direct evidence for the dune migration rate of approximately 1 m yr^{-1}.

ACKNOWLEDGMENTS

The authors would like to thank Dr. Richard Hereford (USGS Flagstaff, Arizona) for his willingness to share long term environmental data, collected from averaging precipitation records from 52 Mojave desert weather stations. The help of Dr. Christopher Earls Brennen, Natalie Becerra, Angel Ruiz-Angulo, Erin Koos and many others, was essential during the field experiments at

Dumont and Eureka dunes. Travel and equipment support for N. M. V. was provided through funding from the Pieter Langerhuizen Lambertuszoon Fonds.

REFERENCES

Bagnold, R.A., 1941. *The Physics of Blown Sand and Desert Dunes,* Dover Publications, London.

Bristow, C.S., Bailey, S.D. & Lancaster, N., 2000. The sedimentary structure of linear sand dunes, *Nature,* **406**(6791), 56–59.

Bristow, C.S., Duller, G.A.T. & Lancaster, N., 2005. Combining ground penetrating radar surveys and optical dating to determine dune migration in Namibia, *J. Geol. Soc.,* **162,** 315–321.

Bristow, C.S., Duller, G.A.T. & Lancaster, N., 2007. Age and dynamics of linear dunes in the Namib Desert, *Geology,* **35**(6), 555–558.

Calkin, P.E. & Rutford, R.H., 1974. The sand dunes of Victoria Valley, Antarctica, *Geogr. Rev.,* **64**(2), 189–216.

Dong, Z., Wang, T. & Wang, X., 2003. Geomorphology of the megadunes in the Badain Jaran Desert, *Geomorphology,* **60**(1-2), 191–203.

Flemming, B.W. & Bartoloma, A., 1995. *Tidal Signatures in Modern and Ancient Sediments,* Blackwell Science, Oxford.

Flenley, E.C., Fieller, N.R.J. & Gilbertson, D.D., 1987. The statistical analysis of "mixed" grain size distributions from aeolian sands in the Libyan Pre-Desert using log skew Laplace models. in *Desert Sediments: Ancient and Modern,* Blackwell Scientific Publications, Oxford.

Grandjean, G., Paillou, P., Dubois, P., August, T., Baghdadi, N. & Achache, J., 2001. Subsurface structures detection by combining L-band polarimetric SAR and GPR data: example of the Pyla dune (France), *IEEE Trans. Geosci. Remote Sens.,* **39**(6), 1245–1258.

Greeley, R. *et al.*, 1995. Potential transport of windblown sand: influence of surface roughness and assessment with radar data. in *Desert Aeolian Processes,* Chapman & Hall, London.

Hereford, R., Webb, R.H. & Longpre, C.I., 2006. Precipitation history and ecosystem response to multidecadal precipitation variability in the Mojave Desert region 1893–2001, *J. Arid Environ.,* **67,** 13–34.

Hunter, R.E., 1977. Basic types of stratification in small eolian dunes, *Sedimentology,* **24**(3), 361–387.

Kocurek, G., 1991. Interpretation of ancient eolian sand dunes, *Annu. Rev. Earth planet. Sci.,* **19,** 43–75.

Kocurek, G.A., 1996. Desert aeolian systems, in *Sedimentary Environments: Processes, Facies, and Stratigraphy,* Blackwell Science, Oxford.

Kocurek, G.A. & Lancaster, N., 1999. Aeolian system sediment state: theory and Mojave Desert Kelso dune field example, *Sedimentology,* **46,** 505–515.

Lancaster, N., 1996. Response of eolian geomorphic systems to minor climate change: examples from the southern Californian deserts, *Geomorphology,* **19,** 333–347.

Livingstone, I., 1987. Grain-size variations on a "complex" linear dune in the Namib Desert, in *Desert Sediments: Ancient and Modern,* Blackwell Scientific Publications, Oxford.

Louge, M.Y., Valance, A., Mint Babah, H., Moreau-Trouve, J.-C., Moctar, A., Dupont, P. & Ouid Ahmedou, D., 2010. Seepage-induced penetration of water vapor and dust beneath ripples and dunes, *J. geophys. Res.,* **115,** 1–14.

MacDonald, A.A., 1966. *The Dumont Dune System of the Northern Mojave Desert California,* San Fernando Valley State College, Northridge, CA.

MacKenzie, F.T., 1964. Geometry of Bermuda calcareous dune cross-bedding, *Science,* **144,** 1449–1450.

McKee, E., 1977. An introduction to the study of global sand seas, *U.S. Geol. Surv. Paper,* **1052**(3), 1–20.

Namikas, S.L. & Sherman, D.J., 1995. A review of the effects of surface moisture content on aeolian sand transport, in *Desert Aeolian Processes,* Chapman & Hall, London.

Nielson, J. & Kocurek, G., 1987. Surface processes, deposits, and development of star dunes: dumont dune field, California, *Geol. soc. Am. Bull.,* **99,** 177–186.

Pavlik, B.M., 1980. Patterns of water potential and photosynthesis of desert sand dune plants, Eureka Valley, California, *Oecologia,* **46**(2), 147–154.

Pavlik, B.M., 1989. Phytogeography of sand dunes in the Great Basin and Mojave Deserts, *J. Biogeogr.,* **16,** 227–238.

Reheis, M.C., Goodmacher, J.C., Harden, J.W., McFadden, L.D., Rockwell, T.K., Shroba, R.R., Sowers, J.M. & Taylor, E.M., 1995. Quaternary soils and dust deposition in southern Nevada and California, *Geol. soc. Am. Bull.,* **107,** 1003–1022.

Reynolds, J.M., 1997. *An Introduction to Applied and Environmental Geophysics,* John Wiley and Sons, Chichester.

Schenk, C.J., Gautier, D.L., Olhoeft, G.R. & Lucius, J.E., 1993. Internal structure of an aeolian dune using ground-penetrating radar, *Int. Assoc. Sedimentologists (Spec. Publ. no. 16),* **16,** 61–69.

Thomas, D.S.G., 1987. Discrimitation of depositional environments using sedimentary characteristics in the Mega Kalahari, central southern Africa, in *Desert Sediments: Ancient and Modern,* Blackwell Scientific Publications, Oxford.

Vriend, N.M., Hunt, M.L., Clayton, R.W., Brennen, C.E., Brantley, K.S. & Ruiz-Angulo, A., 2007. Solving the mystery of booming sand dunes, *Geophys. Res. Lett.,* **34**(16), L16306, doi:10.1029/2007GL030276.

Wasson, R.J. & Hyde, R., 1983. Factors determining desert dune type, *Nature,* **304,** 337–339.

SUPPORTING INFORMATION

Additional Supporting Information may be found in the online version of this article:

Figure S1. Internal structure of the Dumont dune measured with 100 MHz ground penetrating radar, enlarged, without annotations: 2007 September 17, characterized by grainflow cross-strata and deposits. The profile is scaled with the radar velocity such that the time coordinate is approximately equal to the spatial coordinate.

Figure S2. Internal structure of the Dumont dune measured with 100 MHz ground penetrating radar, enlarged, without annotations: 2008 March 24, characterized by a strong superposition bounding surface. The profile is scaled with the radar velocity such that the time coordinate is approximately equal to the spatial coordinate.

Figure S3. Internal structure of the Dumont dune measured with 200 MHz ground penetrating radar, enlarged, without annotations: 2007 May 29, characterized by grainflow cross-strata and deposits. The profile is scaled with the radar velocity such that the time coordinate is twice the spatial coordinate.

Figure S4. Internal structure of the Dumont dune measured with 200 MHz ground penetrating radar, enlarged, without annotations: 2008 June 02, characterized by continuing grainflow cross-strata along the entire length of the windward face. The profile is scaled with the radar velocity such that the time coordinate is twice the spatial coordinate.

Figure S5. Internal structure of the Eureka dune measured with 200 MHz ground penetrating radar, enlarged, without annotations: 2007 October 27, characterized by a rich internal structure. The profile is scaled with the radar velocity such that the time coordinate is twice the spatial coordinate.

Figure S6. Internal structure of the Eureka dune measured with 200 MHz ground penetrating radar, enlarged, without annotations: 2008 July 17, characterized by a rich internal structure. The profile is scaled with the radar velocity such that the time coordinate is twice the spatial coordinate.

Figure S7. Kirchhoff migrated ground penetrating radar data of the Eureka dune on 2007 October 27 for 100 MHz data, enlarged, without annotations.

Figure S8. Kirchhoff migrated ground penetrating radar data of the Eureka dune on 2007 October 27 for 200 MHz data, enlarged, without annotations.

Figure S9. Near-surface velocity structure and internal layering of the Dumont dune, enlarged, without annotations: (a) GPR and seismic of 2007 May 29, (b) GPR of 2007 September 18, (c) GPR of 2008 March 24, (d) GPR and seismic of 2008 June 1. There is some variation in near-surface layering throughout the season, but the general characteristics remain the same.

Figure S10. Near-surface velocity structure and internal layering of the Eureka dune, enlarged, without annotations: (a) GPR and seismic of 2007 October 27 featuring near-surface parallel layer on both faces with deeper tilted layers and (b) GPR and seismic of 2008 July 17 showing strongly tilted layers penetrating to the surface.